the plant journal

A non-canonical function of Arabidopsis ERECTA proteins and a role of the SWI3B subunit of the SWI/SNF chromatin remodeling complex in gibberellin signaling

Elzbieta Sarnowska[1,†], Szymon Kubala[2,†], Pawel Cwiek[2,†], Sebastian Sacharowski[2] (iD), Paulina Oksinska[2], Jaroslaw Steciuk[2], Magdalena Zaborowska[2], Jakub M. Szurmak[2], Roman Dubianski[1], Anna Maassen[2], Malgorzata Stachowiak[1], Bruno Huettel[3], Monika Ciesla[2], Klaudia Nowicka[2], Anna T. Rolicka[2,4], Saleh Alseekh[5,6] (iD), Ernest Bucior[2], Rainer Franzen[7], Anna Skoneczna[2], Malgorzata A. Domagalska[7], Samija Amar[7], Mohammad-Reza Hajirezaei[8], Janusz A. Siedlecki[1], Alisdair R. Fernie[5,6] (iD), Seth J. Davis[7,9,10,*] and Tomasz J. Sarnowski[2,7,*] (iD)

[1]*Maria Sklodowska-Curie National Research Institute of Oncology, Roentgena 5, Warsaw, Poland,*

[2]*Institute of Biochemistry and Biophysics Polish Academy of Sciences, Pawinskiego 5A, Warsaw, Poland,*

[3]*Max Planck Genome Centre Cologne, D-50820, Cologne, Germany,*

[4]*Faculty of Biology, University of Warsaw, Warsaw, Poland,*

[5]*Max Planck Institute of Molecular Plant Physiology, 14476, Potsdam-Golm, Germany,*

[6]*Center for Plant Systems Biology and Biotechnology, 4000, Plovdiv, Bulgaria,*

[7]*Max-Planck Institute for Plant Breeding Research, D-50829, Cologne, Germany,*

[8]*Leibniz-Institut für Pflanzengenetik und Kulturplfanzenforschung Corrensstraße 3 D-06466 Seeland, OT Gatersleben, Germany,*

[9]*State Key Laboratory of Crop Stress Biology, School of Life Sciences, Henan University, 13, Kaifeng 475004, China, and*

[10]*Department of Biology, University of York, York YO10 5DD, UK*

SUMMARY

The *Arabidopsis* ERECTA family (ERf) of leucine-rich repeat receptor-like kinases (LRR-RLKs) comprising ERECTA (ER), ERECTA-LIKE 1 (ERL1), and ERECTA-LIKE 2 (ERL2) controls epidermal patterning, inflorescence architecture, and stomata development and patterning. These proteins are reported to be plasma membrane associated. Here we show that the *er/erl1/erl2* mutant exhibits impaired gibberellin (GA) biosynthesis and perception alongside broad transcriptional changes. The ERf kinase domains were found to localize to the nucleus where they interact with the SWI3B subunit of the SWI/SNF chromatin remodeling complex (CRCs). The *er/erl1/erl2* mutant exhibits reduced SWI3B protein level and affected nucleosomal chromatin structure. Similar to *swi3c* and *brm* plants with inactivated subunits of SWI/SNF CRCs, it also does not accumulate DELLA RGA and GAI proteins. The ER kinase phosphorylates SWI3B *in vitro*, and the inactivation of all ERf proteins leads to the decreased phosphorylation of SWI3B protein *in vivo*. The identified correlation between DELLA overaccumulation and SWI3B proteasomal degradation, and the physical interaction of SWI3B with DELLA proteins indicate an important role of SWI3B-containing SWI/SNF CRCs in gibberellin signaling. Co-localization of ER and SWI3B on *GID1* (*GIBBERELLIN INSENSITIVE DWARF 1*) DELLA target gene promoter regions and abolished SWI3B binding to GID1 promoters in er/erl1/erl2 plants supports the conclusion that ERf-SWI/SNF CRC interaction is important for transcriptional control of GA receptors. Thus, the involvement of ERf proteins in the transcriptional control of gene expression, and observed similar features for human HER2 (epidermal growth family receptor member), indicate an exciting target for further studies of evolutionarily conserved non-canonical functions of eukaryotic membrane receptors.

Keywords: *Arabidopsis*, ERECTA, SWI3B, SWI/SNF, HER2, chromatin, DELLA.

INTRODUCTION

The ERECTA family (ERf) of leucine-rich-repeat receptor-like kinases (LRR-RLKs) consists of three members: ERECTA (ER), ERECTA-LIKE 1 (ERL1), and ERECTA-LIKE 2 (ERL2). ERf proteins carry extracellular LRRs, as well as transmembrane and cytosolic kinase domains (Kosentka et al., 2017; Shpak et al., 2004; Torii et al., 1996). *ERECTA* mutants display developmental defects in inflorescence, pedicel, and silique compaction, while the individual loss of either *ERL1* or *ERL2* function has a limited effect on *Arabidopsis thaliana* L. development (Shpak et al., 2004). ERf proteins are functionally redundant. However, their simultaneous inactivation results in dramatic growth retardation, severe dwarfism, enlargement of the shoot apical meristem, clustered stomata, and sterility. The ERf affect stem cell homeostasis via buffering cytokinin responsiveness and auxin perception in shoot apical meristem and modulating the balance between stem cell proliferation and consumption (Chen et al., 2013; Griffiths et al., 2006; Shpak, 2013; Shpak et al., 2004; Torii et al., 2007; Uchida et al., 2013; Zhang et al., 2021). ERECTA controls the expression of genes associated with gibberellin (GA) metabolism (Uchida et al., 2012) restricting xylem expansion downstream of the GA pathway (Ragni et al., 2011). They also coordinately influence shade avoidance in a GA and auxin-dependent manner (Du et al., 2018) and ethylene-induced hyponastic growth (Van Zanten et al., 2010).

Overexpression of an ER variant lacking the C-terminal kinase domain (ERΔK) caused more severe developmental defects than complete inactivation of *ERECTA*, suggesting an interaction of the kinase domain with important regulatory partners (Shpak, 2003). ERECTA interacts with ERL1 and ERL2 to form receptor complexes recognizing two endodermis-derived peptide hormones (EPFL4 and EPFL6), affecting vascular differentiation and stem elongation. ERf proteins additionally form complexes with the receptor-like protein TOO MANY MOUTHS, which affects stomatal differentiation by recognition of the secretory peptides EPIDERMAL PATTERNING FACTOR 1 (EPF1), EPF2, and stomagen (Lee et al., 2012; Lee, Hnilova, et al., 2015; Uchida et al., 2012).

ERL2 has been found to undergo endocytosis (Ho et al., 2016), suggesting that ERf proteins may play, as yet uncharacterized, important roles upon internalization, in addition to their functions as ligand-binding membrane receptors. ERECTA signaling, in tandem with the SWR1 chromatin remodeling complex (CRC), controls the expression of the *PACLOBUTRAZOL RESISTANCE 1* (*PRE1*) family genes. This observation supports their role in the GA signaling pathway; however, neither direct interaction between ERECTA and SWR1 nor the direct influence of ERECTA signaling on chromatin structure or SWR1 activity

has, as yet, been demonstrated (Cai et al., 2017; Cai et al., 2021).

Here we show that the genetic loss of all ERf proteins in the *er/erl1/erl2* triple mutant (*erf*) results in broad transcriptomic changes affecting hormonal, developmental, and metabolic processes. Inactivation of ERf proteins caused downregulation of the GA receptor *GID1* (*GIBBERELLIN INSENSITIVE DWARF 1*) gene expression and decreased bioactive GA levels. The *er/erl1/erl2* plants are unable to accumulate RGA and GAI DELLA proteins and exhibit decreased expression of genes encoding DELLA repressors. The ER protein undergoes endocytosis and enters the nucleus. All three ERf proteins interact in the nucleus with the SWI3B core subunit of the SWI/SNF CRCs. The kinase domain of the ER protein exhibits the ability to phosphorylate SWI3B protein. The physical interaction of SWI3B with RGA and RGL1, together with identified correlation between DELLA accumulation, SWI3B proteasomal degradation and with the role of ERf in SWI3B phosphorylation justify the important role of SWI3B-containing SWI/SNF CRCs in GA signaling. The ER and SWI3B also co-localized in the promoter regions of *GID1* DELLA target genes. In the *erf* mutant, the binding of SWI3B to *GID1* promoters was abolished suggesting that ERf proteins directly control GA receptor expression by restricting recruitment of the SWI/SNF CRCs to its target *loci*. Our data collectively suggest cooperation of ERf signaling with SWI/SNF in the modulation of the GA gene expression network.

RESULTS

Inactivation of *ERf* proteins has a broad effect on the *Arabidopsis* transcriptome including GA signaling

The *Arabidopsis er/erl1/erl2* plants exhibit severe dwarfism, dark green color, defects in vascular development, stem elongation, stomatal differentiation, and complete sterility (Figure 1a, Figure S1a; Shpak et al., 2004). Given the severe phenotypic alterations of the *er/erl1/erl2* plants, we performed transcript profiling with Affymetrix ATH1 microarrays on RNA samples from aerial parts of the *er/erl1/erl2* mutant and wild type (WT) adult plants (representing the most comparable stage of the development) grown for 5 weeks under long-day conditions (16 h day/8 h night). Data analysis identified 1734 versus 1680 genes showing a >1.50-fold decrease and increase, respectively, of transcript levels in *er/erl1/erl2* compared with WT (Figure S1b; Data S1, Sub-Tables S1 and S2). Gene Ontology (GO) terms of primary metabolism, developmental processes, and response to hormones were enriched among the *er/erl1/erl2* downregulated genes (Data S1, Sub-Table S3). Among these, 27 genes were classified as being involved in the GA response (Table S1; Data S1, Sub-Tables S1 and S3). The upregulated genes were
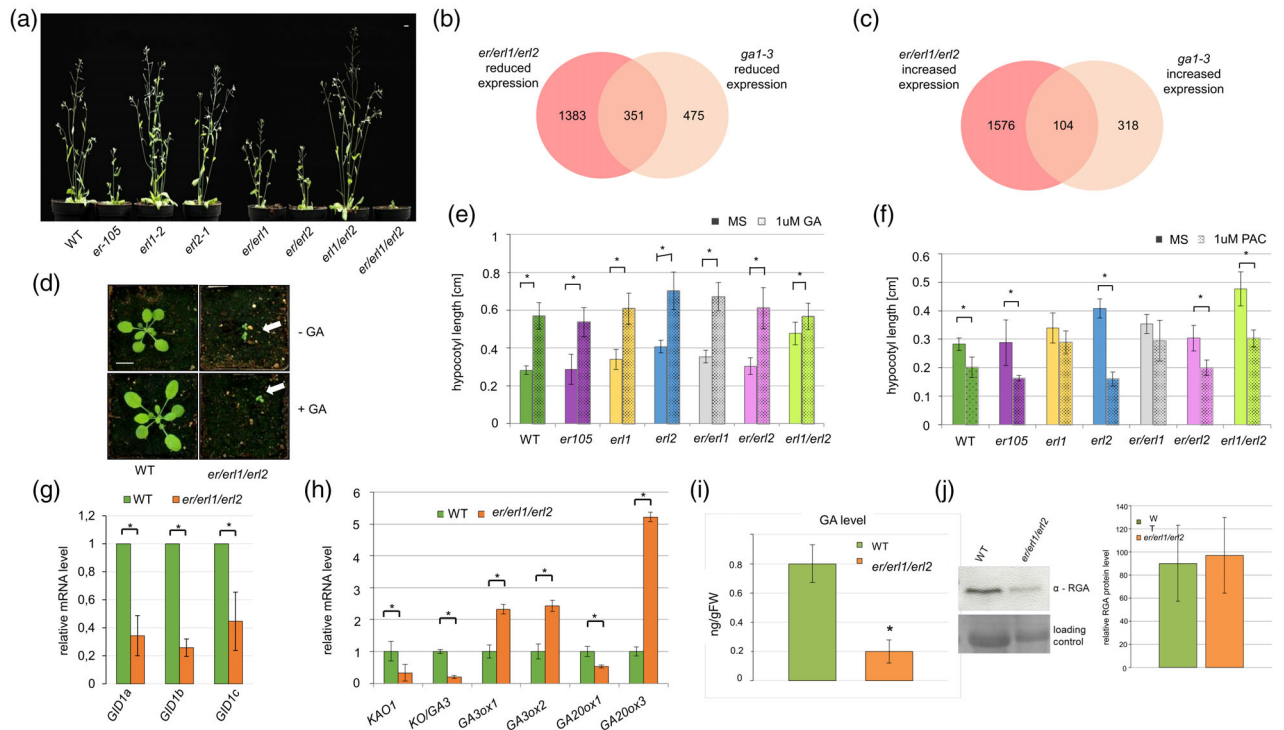
Figure 1. ERf inactivation affects Arabidopsis development, causes transcriptomic changes overlapping with the effect of *ga1-3* mutation and impairs gibberellin (GA) biosynthesis and signaling.

(a) Phenotypic changes conferred by combinations of *erf* mutations. Scale bar = 1 cm.

(b) Overlapping downregulated genes in *er/erl1/erl2* and *ga1-3* plants.

(c) Overlapping upregulated genes in *er/erl1/erl2* and *ga1-3* plants.

(d) *er/erl1/erl2* plants exhibit impaired GA response. 14-day-old long days (12 h day/12 night) grown wild type (WT) and er/erl1/erl2, sprayed twice a week with water (upper row) or 100 μм GA4 + 7 (lower row). Arrows: *er/erl1/erl2* plants. Scale bar = 1 cm.

(e) The GA response is retained to various levels in combinations of erf mutants. Error bars refer to SD,*$P < 0.05$, Student's *t*-test, $n = 30$ plants.

(f) Response of various *erf* mutants to 1 μм paclobutrazol treatment. Error bars refer to SD,*$P < 0.05$, Student's *t*-test, $n = 30$ plants.

(g) *er/erl1/erl2* mutant exhibits altered transcription of GID1 GA receptor genes (error bars refer to SD, $P < 0.05$, Student's *t*-test, three biological and technical replicates were assayed).

(h) *er/erl1/erl2* mutant displays altered GA biosynthesis and metabolism-related genes expression (error bars refer to SD, $P < 0.05$, Student's *t*-test, three biological and technical replicates were assayed).

(i) *er/erl1/erl2* mutant exhibits dramatically reduced level of bioactive GA$_{4 + 7}$ gibberellin (error bars refer to SD, $P < 0.05$, Student's *t*-test, three biological and technical replicates were assayed).

(j) *er/erl1/erl2* mutant does not accumulate the DELLA protein RGA, the relative RGA protein level was quantified using ImageJ software from four independent Western blot experiments.

classified into GO-terms of chloroplast-related metabolic and light-regulated transcription processes, responses to cytokinin, and auxin degradation (Data S1, Sub-Tables S2 and S4). Several genes acting in leaf epidermal and stomatal cell differentiation showed enhanced expression in the *er/erl1/erl2* mutant (Table S2). In conclusion, the inactivation of ERf altered transcriptional regulation of hundreds of targets, including a set of GA-regulated genes.

Phenotypic traits exhibited by double and triple *erf* mutants resemble those of double and triple *gid1abc* (*gibberellin insensitive dwarf 1a, b,* and *c*) plants (Figure 1a; Griffiths et al., 2006). Inactivation of *GID1abc* genes has a nearly identical effect on the *Arabidopsis* transcriptome as the severe GA-deficient mutant *ga1-3* (Willige et al., 2007).

We compared the transcriptomic data available for the *ga1-3* mutant with those caused by inactivation of all *ERf* genes. This identified a large overlap of differentially expressed genes in the *er/erl1/erl2* and *ga1-3* lines. Among 826 genes downregulated in the *ga1-3* line, 351 (about 42.5%) also exhibited decreased expression in the *er/erl1/erl2* plants (Figure 1b), while 104 genes (about 24.6% of *ga1-3* upregulated genes) were upregulated in both lines (Figure 1c). Only 33 genes were upregulated in *ga1-3* but downregulated in *er/erl1/erl2* (Figure S1c), and only 64 genes downregulated in *ga1-3* but upregulated in *er/erl1/erl2* (Figure S1d). Differentially expressed genes common to *ga1-3* and *er/erl1/erl2* lines belonged to both DELLA (repressors of GA pathway)-dependent and DELLA-independent classes (Cao et al., 2006), regardless of whether they display co-regulation or contrasting regulation in these lines (Figure S1e,f). This suggests the involvement of *Arabidopsis* ERf proteins in the mediation of GA-

related processes. Therefore, we next tested the response of *er/erl1/erl2* plants to exogenously supplied bioactive 100 μM GA$_{4+7}$ and found that spraying of the *er/erl1/erl2* mutant grown under long day conditions (12 h day/12 h night) did not lead to increased leaf size by day 14 compared with the remarkable expansion of control WT rosette leaves (Figure 1d; Figure S2a). Thus *er/erl1/erl2* displayed GA insensitivity. Nonetheless, the GA treatment resulted in bolting of *er/erl1/erl2* plants, only after over 2 months (Figure S2b,c), indicating their residual response to GA.

Although we showed that ERf proteins are involved in the GA response, it remained unclear whether proper GA perception requires all ERf proteins. Thus, we tested the hypocotyl response of single and double *erf* mutants in various combinations to the treatment with 1 μM GA$_{4+7}$ or 1 μM paclobutrazol (PAC), an inhibitor of GA biosynthesis. The GA response was retained to various levels in all tested mutants (Figure 1e) while the *erl1* and *er/erl1* plants had an impaired response to PAC and *erl1/erl2* displayed a significant reduction of hypocotyl length (Figure 1f).

Upon crossing *er*, *er/erl1*, and *er/erl2* lines with the *ga1-3* mutant, we observed only a discrete enhancement of the *ga1-3* phenotype. However, most of the phenotypic changes characteristic of *ga1-3* mutation were retained, indicating that many of the *er*, *erl1*, or *erl2* single or double mutant phenotypes are likely not exclusively a result of GA deficiency (Figure S2d,e).

We have shown that only parallel inactivation of all ERf proteins causes severe impairment of the GA response. Quantitative real-time polymerase chain reaction (PCR) measurements of GA response and biosynthesis genes expression revealed a parallel 2.5–3-fold reduction in the transcript levels of all three *GID1* GA receptors in the *er/erl1/erl2* mutant compared with WT (Figure 1g). The GA-receptor genes *GID1A/B* have been reported to be direct chromatin immunoprecipitation (ChIP) targets of RGA, a major DELLA repressor of GA signaling, which stimulates *GID1* transcription (Zentella et al., 2007). The *er/erl1/erl2* triple mutant also displayed altered expression of GA biosynthesis genes compared with the WT: a four-fold reduction of mRNA levels of *KAO1* (*ent*-kaurenoic acid oxidase) and *KO* (*ent*-kaurene oxidase), a 2.5-fold increase of mRNA levels of GA-repressed *GA3ox1* and *GA3ox2* (GIBBERELLIN 3 BETA-HYDROXYLASE 1 and 2), a two-fold inhibition and five-fold upregulation, respectively, of mRNA levels corresponding to the *GA20ox1* and *GA20ox3* genes (Figure 1h). This indicated that the ERf proteins influence not only the expression of GA receptors, but also genes associated with GA biosynthesis. We subsequently found a substantial decrease of bioactive GA$_4$ as well as GA$_{12}$, and GA$_{24}$ intermediates in *er/erl1/erl2* mutant (Figure 1i; Figure S3a). Counterintuitively, Western blotting using a specific antibody (Willige et al., 2007) detected lack of accumulation of

RGA and GAI DELLA proteins in the *er/erl1/erl2* mutant plants (Figure 1j; Figure S3b) although they resemble plants with impaired GA pathway and exhibit decreased bioactive GA$_4$ levels. We next performed quantitative real-time PCR measurements of transcript levels for all DELLA genes [*REPRESSOR OF GA1-3 1* (*RGA*), *RGA-LIKE 1–3* (*RGL1-3*), and *GIBBERELLIC ACID INSENSITIVE (GAI)*] and found that their expression was reduced from 1.5 to about two-fold in triple *er/erl1/erl2* plants (Figure S3c), which may support the lack of accumulation of RGA and GAI DELLA proteins in *er/elr1/erl2*. Our results indicate that the parallel inactivation of all ERf proteins results in co-ordinate deregulation of GA biosynthesis and response pathways in Arabidopsis.

ERECTA (ER) protein undergoes endocytosis and migrates to the nucleus

By analogy to some human membrane receptors internalizing to endosomes and migrating to the nucleus (i.e., Giri et al., 2005), the ERL2 member of the ERf undergoes endocytosis (Ho et al., 2016). We next examined, in detail, the cellular localization of ER by creating C-terminal GFP fusions with ER (Figure 2a) after verifying genetic complementation of the *er-105* mutation by a 35S::ER-GFP construct (Figure S4). As observed earlier (Shpak et al., 2005; Uchida et al., 2012), a pool of the ER-GFP protein was detected in association with plasma membranes of the leaf epidermis. In addition, a weak localization signal was detected in internal structures, which could represent endosomes (Figure 2a). In guard cell pairs, the ER-GFP protein was also detected in circles around the positions of nuclei, which were visualized by propidium iodide staining (Figure S5a and Movie S1). We also observed with considerable frequency ER protein in the nuclei of roots of 14–17-day-old *Arabidopsis* plants (Figure 2b); however, ER was mainly located in the plasma membrane and endosome-like structures (Figure 2c).

To verify that the ER-GFP protein indeed undergoes endocytosis, we examined its localization in *Arabidopsis* seedlings treated with 25 μM Brefeldin A (BFA), a compound preventing Golgi-mediated vesicular transport of membrane proteins to the plasma membrane (Miller et al., 1992). We observed accumulation of the ER-GFP protein in BFA bodies within 30–40 min after BFA treatment leading to its accumulation at the nuclei periphery 120 min after BFA application (Figure 2d; Figure S5b). The 4-h long 200 nM leptomycin B treatment (a compound blocking nuclear export by EXPORTINS; Haasen et al., 2002) resulted in the ER accumulation in the cell nuclei (Figure 2e,f). ER thus appeared to behave similarly to certain human plasma-membrane receptors in migrating into the nucleus (Chen & Hung, 2015; Hung et al., 2008).

We noted that ERL1 and ERL2 proteins carry a monopartite nuclear localization signal (NLS) sequence in their
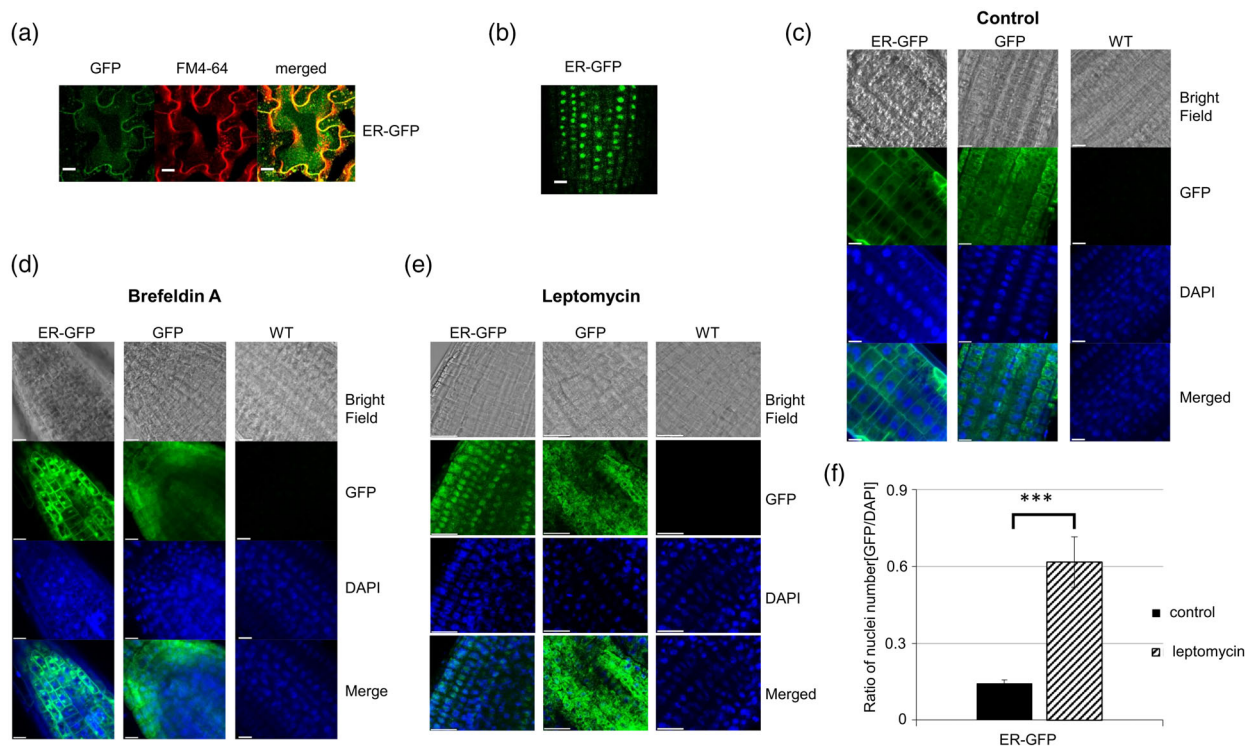
Figure 2. Subcellular localization of ERECTA protein.

(a) ERECTA is localized in plasma membrane and endosomes in epidermal cells of 7-days old seedlings. ER-GFP, or free GFP visualized using GFP channel. FM4-64 specifically stains plasma membranes. Scale bar = 10 μm.

(b) Root-tip images of approximately 2-week-old (14–17 days) ER-GFP seedlings showing nuclear localization of ERECTA protein at considerable frequency.

(c) Root-tip images of 12-day-old ER-GFP seedlings serving as the control for (d) and (e). DAPI, 4′,6-diamidino-2-phenylinodole; WT, wild type.

(d) Brefeldin A treatment enhanced the localization of ERECTA protein in Brefeldin A bodies. Roots of 12-day-old Arabidopsis seedlings.

(e) Leptomycin B treatment enhanced the nuclear localization of ERECTA free GFP was used as a control in (c–e), cell nuclei were stained with DAPI, scale bar = 50 μm.

(f) Leptomycin B enhances nuclear presence of ER protein. The GFP/DAPI ratio calculated per area for roots of plants expressing ER-GFP protein.

kinase domains, while the ERL1 kinase domain carries an additional bipartite NLS identified using cNLS Mapper (Kosugi et al., 2009). The NLS signal in the ER protein was not recognized; however, all ERf proteins show evolutionally conserved amino acid sequences in this region (Figure S6a). Using the NetNES1.1 server (La Cour et al., 2004), we predicted the existence of specific for AtXPO1/ AtCRM1 exportin (Haasen et al., 2002) leucine-rich nuclear export signals (NES) in all ERf proteins (Figure S6a). The subsequent Western blotting analysis of nuclear extracts confirmed the nuclear presence of ER, with the purity of the nuclear fraction being tested using anti-H + ATPase antibody-a marker of the plasma membrane (Figure S6b). In addition to the expected full-length forms (140 kDa), we also detected shorter (approximately 75 kDa) versions of the ERECTA protein with the C-terminal GFP tag and smaller products of degradation, including free GFP, suggesting an analogy to the human epidermal growth factor receptor (EGFR), (Chen & Hung, 2015). The detection of N-terminally truncated forms of the ERECTA protein carrying a kinase domain resembled the recently reported fate of

the XA21 LRR-RLK immune receptor in rice (Park & Ronald, 2012), where its C-terminal kinase domain enters the nucleus to interact with the OsWRKY62 transcriptional regulator.

To assess whether the ERECTA kinase domain (KDER) is imported into the nucleus, we fused the C-terminal part of ERECTA, harboring the KDER, to a YFP-HA tag (Figure S6c) and expressed this construct in the *er-105* mutant. The presence of KDER-YFPHA was detected exclusively in cell nuclei (Figure 3a). Furthermore, KDER-YFPHA expression partially restored the *er-105* rosette and cauline leaf phenotype to WT values (Figure S7a,b). Still, it failed to complement genetically the defect of stem elongation (Figure S7c). Partial genetic complementation of the *er-105* mutation and nuclear localization of KDER prove that the KDER has a receptor-domain independent signaling function. Interestingly, by contrast to the full length and kinase domain of ERECTA protein (Figure 3a), truncated ERΔkinase form of ERECTA protein fused to YFP-HA (ΔKDER-YFP-HA) did not enter into the nucleus proving the presence of functional NES and NLS sequences in the C-terminal part of ERECTA protein.
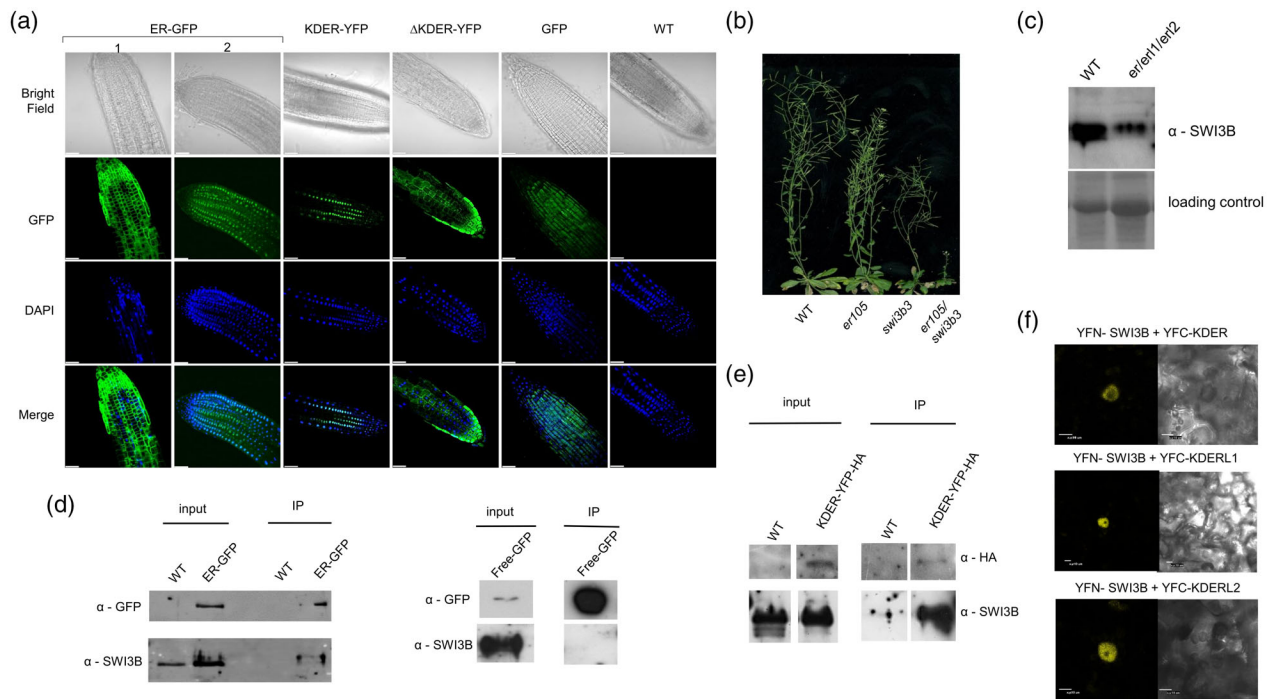
Figure 3. Nuclear function of ERf proteins.

(a) Root-tip images of approximately 2-week-old (14–17 days) plants expressing ER-GFP, KDER-YFP-HA (the kinase domain of the ER protein), ERΔK-YFPHA (truncated ER protein lacking the kinase domain) proteins indicating that the kinase domain is necessary for the nuclear localization of ER protein. Wild-type (WT) and GFP expressing plants-negative controls. Panel 2 in the ER-GFP indicates nuclear localization of ER protein appearing at considerable frequency in untreated plants. Cell nuclei were stained with 4′,6-diamidino-2-phenylinodole (DAPI). Scale bar = 25 μm.

(b) *er-105/swi3b3* double mutant shows more retarded growth than either *er-105* or *swi3b3* plants. Scale bar = 1 cm.

(c) *er/erl1/erl2* triple mutant exhibits reduced SWI3B protein level.

(d) ER-GFP or free GFP (negative control) pull-down from the nucleus and anti-SWI3B Western blotting indicate a specific ER-SWI3B interaction. IP, immunoprecipitation.

(e) IP of KDER-YFP-HA from the nucleus indicated that the kinase domain of ER interacts with SWI3B.

(f) ER, ERL1, and ERL2 kinase domains interact with SWI3B in the nucleus. Bimolecular fluorescence complementation assay in epidermis of tobacco leaves. Scale bar = 10 μm.

Upon nuclei fractionation (Sarnowski et al., 2002), the ERECTA protein was detected in the nuclear membrane, soluble nuclear-protein fraction, and chromatin, with its major presence within the nuclear matrix. The nuclear fractions contained both full-length and N-terminally truncated ER forms (Figure S8), which suggests that ER could be involved in either transcriptional regulation or other nuclear functions.

ERf proteins physically interact with the SWI3B core subunit of SWI/SNF CRC

The weak *swi3b-3* allele (Sáez et al., 2008) carrying a point mutation in the *SWI3B* gene encoding a core subunit of the SWI/SNF CRC, in the *er-105* background, exhibit severe dwarfism, altered leaf shape, delayed flowering, and reduced fertility (Figure 3b). We, therefore, introgressed the *swi3b-3* mutation into WT and found that the phenotypic alterations related to *swi3b-3* were much weaker (slight reduction of growth rate, leading to decreased plant height; Figure 3b) than the phenotypic traits exhibited by

the *er-105/swi3b-3* as well as single *er-105* mutation. The severe phenotypic alterations exhibited by the *er-105/swi3b-3* plants indicated the likely existence of a strong genetic interaction between the ERECTA signaling pathway and SWI3B-containing SWI/SNF CRCs. This observation is in line with (i) the direct binding of 15 of 27 potential ERf target genes related to the GA signaling pathway (Table S1) by SWI/SNF CRCs (Archacki et al., 2016; Li et al., 2016; Sacharowski et al., 2015); (ii) the unexpected broad transcriptional changes and severe effects on *Arabidopsis* development and hormonal signaling pathways observed in the *er/erl1/erl2* mutant; and (iii) the well-recognized function of SWI/SNF CRC in the interface of hormonal signalling pathway including impairment of GA signaling and direct interaction of SWI3C subunit with DELLA and SPINDLY proteins (Sarnowska et al., 2013; Sarnowska et al., 2016).

We next assessed the level of the SWI3B protein in *er/erl1/erl2* plants. We found a significant decrease in the SWI3B protein abundance (Figure 3c), further suggesting
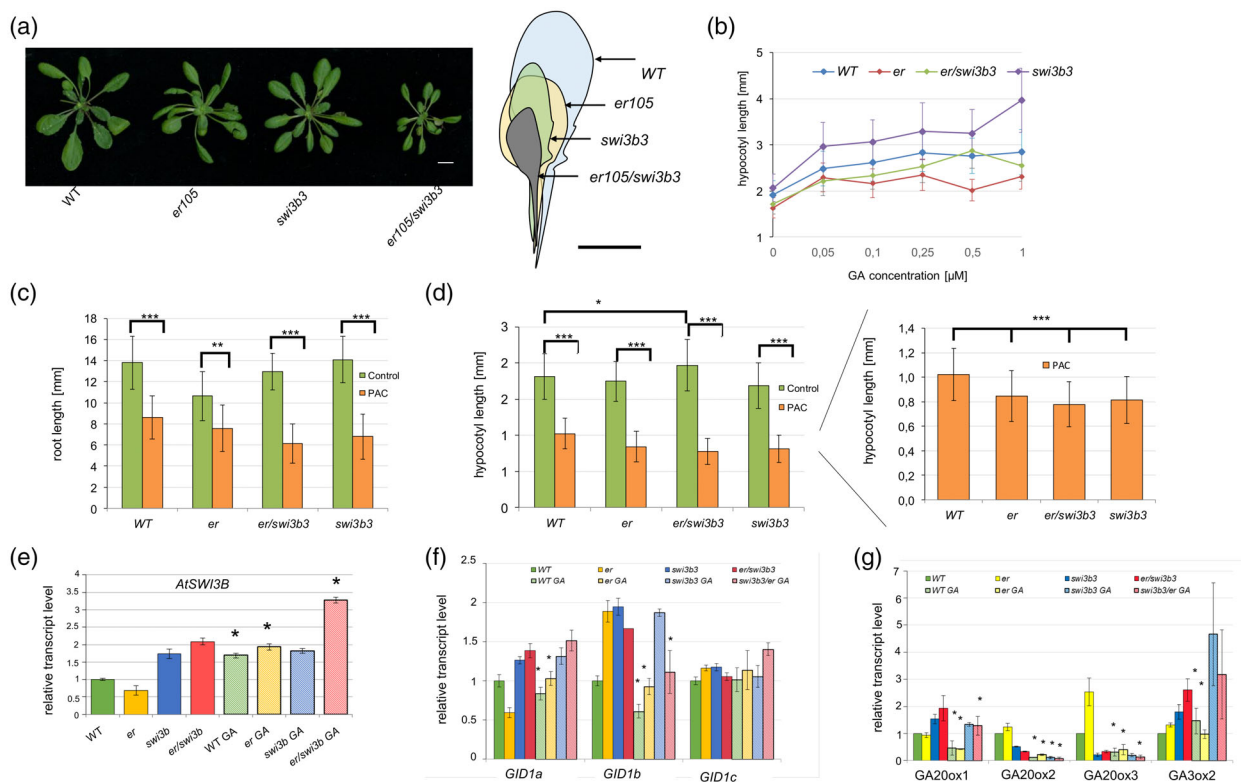
Figure 4. ER and SWI3B interact genetically and affect both gibberellin (GA) biosynthesis and response pathways.

(a) *er-105/swi3b-3* double mutant exhibits more retarded growth than the *er-105* and *swi3b-3* (3-week-old plants). Graphical alignment of corresponding leaves. Scale bar = 1 cm.

(b) Hypersensitivity of 1-week-old *swi3b-3* hypocotyl to GA treatment is abolished by introducing *er-105*.

(c) Roots of all tested 1-week-old genotypes similarly respond to paclobutrazol (PAC) treatment (error bars refer to SD, *$P < 0.01$,**$P < 0.001$, ***$P < 0.0001$, Student's *t*-test). *pI*, isoelectric point; WT, wild type.

(d) Hypocotyls of all tested 1-week-old genotypes similarly respond to PAC treatment, right panel- hypocotyl length comparison for PAC treated plants only (error bars refer to SD, *$P < 0.01$,**$P < 0.001$, ***$P < 0.0001$ Student's *t*-test).

(e) *swi3b-3* weak, point mutant line and *er-105/swi3b-3* exhibit elevated SWI3B transcript level, the SWI3B expression is elevated after supplementation with bio-active $GA_{4 + 7}$ in all genotypes except *swi3b-3* (error bars refer to SD, $P < 0.05$, Student's *t*-test).

(f) Examination of *GID1* genes indicated that almost all examined lines responded to GA treatment, but the *swi3b-3* line was insensitive for GA-induced transcriptional changes (error bars refer to SD, $P < 0.05$, Student's *t*-test).

(g) Examination of GA biosynthesis genes indicated that almost all examined lines responded to GA treatment, but the *swi3b-3* line was insensitive for GA-induced transcriptional changes except *GA20ox2* expression (error bars refer to SD, $P < 0.05$, Student's *t*-test).

that the ERf signaling pathway may influence the proper function of SWI3B-containing SWI/SNF CRCs. In addition, the SWI3B was found to bind ER-GFP but not free GFP (Figure 3d). Similarly, co-immunoprecipitation indicated that SWI3B interacts with the kinase domain of ER (Figure 3e).

Next, we performed bimolecular fluorescence complementation assay (BiFC) assays (Hu et al., 2002) in epidermal cells of *Nicotiana benthamiana* and confirmed the SWI3B and ER kinase domain interaction. The YFC-RFP served as a control unrelated protein with broad intracellular localization (Figure 3f; Figure S9). We also detected the interaction of SWI3B with the kinase domain of the ERL1 or ERL2 (Figure 3F; Figure S9), indicating the existence of direct interdependences between the ERf signaling pathway and SWI/SNF-dependent chromatin remodeling.

Moreover, we found similar interactions in the nuclei of human cells for HER2 (EGFR family member), a membrane receptor acting in a non-canonical signaling mode, including translocation to the nucleus (Lee, Wang, & Hung, 2015), and BAF155 a SWI3-type subunit of human SWI/SNF CRCs (Figure S10, Method S1). Thus, our data indicate that the phenomenon observed for ERf and SWI3B is not limited to *Arabidopsis* but rather may be a general feature of SWI/SNF CRCs and membrane receptors.

ERECTA and *SWI3B* interact genetically and *er/elr1/erl2* plants exhibit alteration in chromatin status

The *er-105/swi3b-3* double mutant exhibited more severe phenotypic traits than both single *er-105* and *swi3b-3* mutant lines (Figure 4a), supporting the observed physical interdependences between ER and SWI3B.

© 2023 The Authors.

Treatment with bioactive GAs, GA$_{4+7}$, indicated hypersensitivity of *swi3b-3* to GA demonstrated by hypocotyl length, while the response of *er-105* was reduced. By contrast, the GA hypersensitivity of *swi3b-3* was abolished by introduced *er-105* mutation (Figure 4b). All tested genotypes were responding to PAC treatment in a similar way (Figure 4c,d). The higher expression of *SWI3B* was visible in the case of the *swi3b-3* mutant, which was even more pronounced in *er-105/swi3b-3* (Figure 4e). The expression of *SWI3B* was elevated after supplementation with bioactive GAs, GA$_{4+7}$, in all genotypes, except for the *swi3b-3* line (Figure 4e). The examination of *GID1* and GA biosynthesis genes indicated that almost all examined lines responded to GA treatment while the *swi3b-3* line was insensitive for induced by GA transcriptional changes observed for other genotypes, except for *GA20ox2* expression (Figure 4f,g). Collectively, our results further indicate that both ERf signaling and SWI3B-containing CRCs play together an important role in the fine-tuning of GA signaling in Arabidopsis.

To verify the biological effect of observed interactions between ERf signaling and SWI3B-SWI/SNF, we analyzed the chromatin status, nuclei shape, and chromocenter number in the *er/erl1/erl2* mutant plants. We found that *er/erl1/erl2* plants exhibit increased chromocenter number and altered spindle-like nuclei shape (Figure S11a,b). Furthermore, we screened the effect of inactivation of ERf on genome-wide nucleosome positioning in chromatin using *micrococcal nuclease* protection assays followed by deep sequencing (MNase-seq) and confirmatory MNase-quantitative PCR in WT and *er/erl1/erl2* plants. We found that inactivation of ERf proteins has a broad influence on the global nucleosomal chromatin structure in *Arabidopsis-erf* exhibited 41 519 nucleosome occupancy changes, 13 924 "fuzziness" changes and 4055 nucleosome position changes (Figure S12a) and alterations in the presumable regulatory regions upstream of the transcription start site (TSSs) (Figure S12b, Data S1, Sub-Tables S9–S14; Method S2).

Among genes with downregulated expression and altered nucleosome positioning in the *er/erl1/erl2* mutant identified using microarray analysis and quantitative real-time PCR measurements we found 15 GA-related genes (*ATBETAFRUCT4, XERICO, PRE1, MYBR1, MYB24, MIF1, HAI2, ZPF6, GA20ox1, CGA1, XTH24, GID1a, GID1b, RGL1,* and *GIS3*) Interestingly, eight of them (*ATBETAFRUCT4, PRE1, MYBR1, MIF1, XTH24, GID1a, GID1b,* and *RGL1*) were already observed to be directly targeted by the BRM ATPase of the SWI/SNF CRC (Archacki et al., 2016; Li et al., 2016). An Integrated Gene Browser view of *PRE1, GID1a,b* promoter regions indicated (Figure S12d) various nucleosome alterations on promoter regions of these genes in the *er/erl/erl2* mutant pointing out impaired chromatin remodeling in the absence of functional ERf proteins. The selected changes were confirmed by MNase-quantitative PCR (Figure S12e).

Inactivation of ERf proteins affects SWI3B protein phosphorylation

We next tested the capacity of KDER to phosphorylate SWI3B protein. We purified, and subsequently used MBP-His6-KDER and His6-SWI3B (Figure 5a; Figure S13a) for non-radioactive *in vitro* kinase assay. The existence of a strong band corresponding to phosphorylated SWI3B protein and a weaker band of autophosphorylated KDER was indicated (Figure 5b; Figure S13b,c). The confirmatory mass-spectrometry analysis resulted in the identification of the active phosphorylation sites at KDER and in the SWI3B protein (Figure S13d,e). Interestingly, three of four KDER-dependent phosphorylation sites were located in SWI3B in SWIRM and SANT domains (Figure S13e,f), providing a valuable hint that the ERf family proteins may be responsible for the SWI3B phosphorylation.

To verify this possibility, *in vivo* phosphorylation analysis using 2D-isoelectrofocusing (IEF)-polyacrylamide gel electrophoresis combined with the Western blot was performed. The alteration in the SWI3B proteins isoelectric point (*pI*) in *er/erl1/erl2* mutant was observed. The bands corresponding to phosphorylated SWI3B form were nearly absent in *er/erl1/erl2* plants, indicating a severe defect in SWI3B phosphorylation (Figure 5c). These data strongly support the regulatory function of the ERf proteins on the SWI3B subunit of SWI/SNF CRC.

Accumulation of DELLA proteins correlates with increased proteasomal degradation of SWI3B

Our previous study demonstrated that SWI3C, a partner of SWI3B, physically interacts with DELLA proteins (Sarnowska et al., 2013). We also found that the *Arabidopsis* lines with impaired SWI/SNF CRC-*brm* and -*swi3c* exhibit a decreased level of bioactive GA$_4$ (Archacki et al., 2013; Sarnowska et al., 2013). Similarly to the case of *er/erl1/erl2* mutant plants, they do not accumulate RGA and GAI DELLA proteins (Figure S14; Figure 1j and Figure S3b) and *swi3c* plants exhibit decreased DELLA transcript levels (Sarnowska et al., 2013). To investigate deeper if SWI3B function may be related to defects in GA signaling exhibited by *er/erl1/erl2* plants, we used a BiFC assay to analyze the interaction between DELLA and SWI3B. The interaction between either RGA or RGL1 protein and SWI3B was found (Figure 5d; Figure S15). No YFP signal was detected in control cells.

To understand the functional consequences of the detected interactions between SWI3B and DELLA proteins, we analyzed the amounts of SWI3B and RGA proteins in GA or PAC-treated plants (Figure 5e). Surprisingly, we observed the PAC-dose-dependent disappearance of SWI3B protein (Figure 5f). To check if the degradation of SWI3B under these conditions depended on the proteasome, we tested the effect
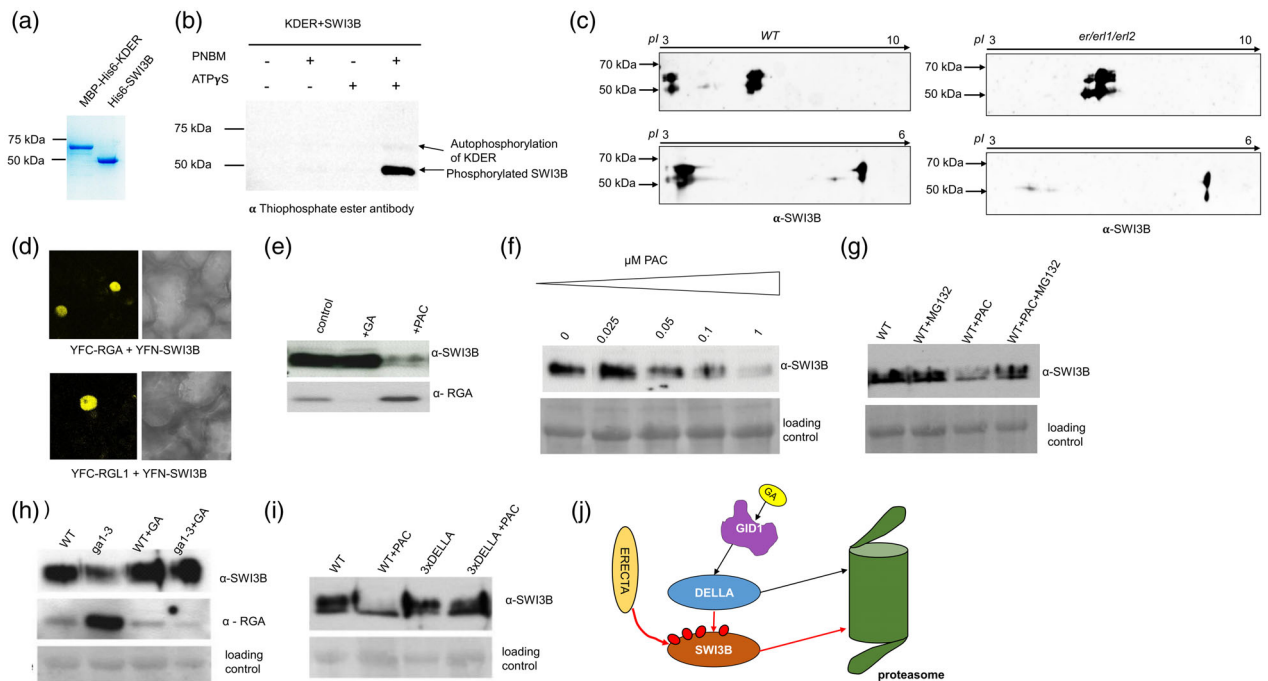
Figure 5. ERf proteins are responsible for the phosphorylation of SWI3B protein, while RGA a DELLA protein controls SWI3B protein levels.

(a) Coomassie staining of MBP-His6-KDER and His6-SWI3B proteins purified from bacteria. WT, wild type.

(b) Western blot with anti-thiophosphate ester antibody showing *in vitro* SWI3B phosphorylation by KDER. GA, gibberellin.

(c) 2D Western blot assay with anti-SWI3B antibody indicating *in vivo* phosphorylation alteration of SWI3B protein in *er/erl1/erl2* mutant. PAC, paclobutrazol.

(d) SWI3B, RGA, and RGL1 proteins in the nuclei of living cells. Bimolecular fluorescence complementation assay in epidermis of tobacco leaves. Scale bar = 10 μm.

(e) Amounts of SWI3B and RGA proteins in plants are oppositely affected by PAC treatment.

(f) Disappearance of SWI3B protein is PAC dose dependent.

(g) PAC-dependent degradation of SWI3B is abolished by the MG132 treatment, a known proteasome inhibitor.

(h) *ga1-3* mutant constitutively accumulating DELLA proteins exhibits the decreased level of SWI3B, which is restored to WT levels upon GA treatment.

(i) Triple DELLA mutant exhibits a WT-like level of SWI3B protein, and the PAC treatment does not influence SWI3B level in this background.

(j) Schematic model highlighting ERf and DELLA impact on the SWI3B protein.

of MG-132 on the SWI3B level. MG-132 treatment caused increasing SWI3B abundance in PAC-treated plants (Figure 5g), suggesting that the degradation of SWI3B observed in parallel to the accumulation of DELLAs did indeed occur via the proteasome. We also observed increased degradation of SWI3B in the *ga1-3* mutant in which DELLA proteins are constitutively accumulated (Figure 5h), but we did not observe enhanced SWI3B degradation in PAC-treated 3xdella (Archacki et al., 2013) collectively suggesting that binding of SWI3B by DELLA proteins may be a primary cause of its proteasomal degradation (Figure 5i,j). This observation is in line with previous reports indicating that DELLA proteins are responsible for sequestration and degradation of some transcription factors and chromatin remodeling factors, i.e., PICKLE a CHD3 type remodeler (Phokas & Coates, 2021; Zhang et al., 2014). Collectively, our results indicate that the SWI3B protein similarly as other subunits of SWI/SNF CRCs (BRM and SWI3C) is involved in GA action in Arabidopsis and provide extended insight into the functioning of the ERECTA family proteins and DELLA proteins, and their mutual impact on the SWI3B-containing SWI/SNF CRCs.

Binding of ERECTA and SWI3B to promoter regions of the *GID1* genes

The *er/erl1/erl2* mutant displays an impaired response to exogenous GA treatment and a consistently decreased expression of all three *GID1* genes. ERf proteins interact with the SWI3B, inactivation of *ERf* proteins results in nucleosomal chromatin structure alterations and decreased abundance of SWI3B and its phosphorylated form in Arabidopsis, and there is an intriguing interdependence between the control of the SWI3B level and DELLA protein accumulation. Therefore, we examined if ER and the SWI3B participate in transcriptional control of the *GID1* genes previously reported as targets for DELLA (La Rosa et al., 2015). The ChIP analysis on *GID1* promoters was performed using nuclei purified from 3-week-old seedlings expressing the ER-GFP and the SWI3B-HIS-STREP-HA proteins. The binding of ER-GFP was detected around −130 bp upstream of the TSS in the *GID1a* promoter region while SWI3B bound around the TSS of the *GID1a* promoter (Figure 6a). The ER protein was targeted to two regions
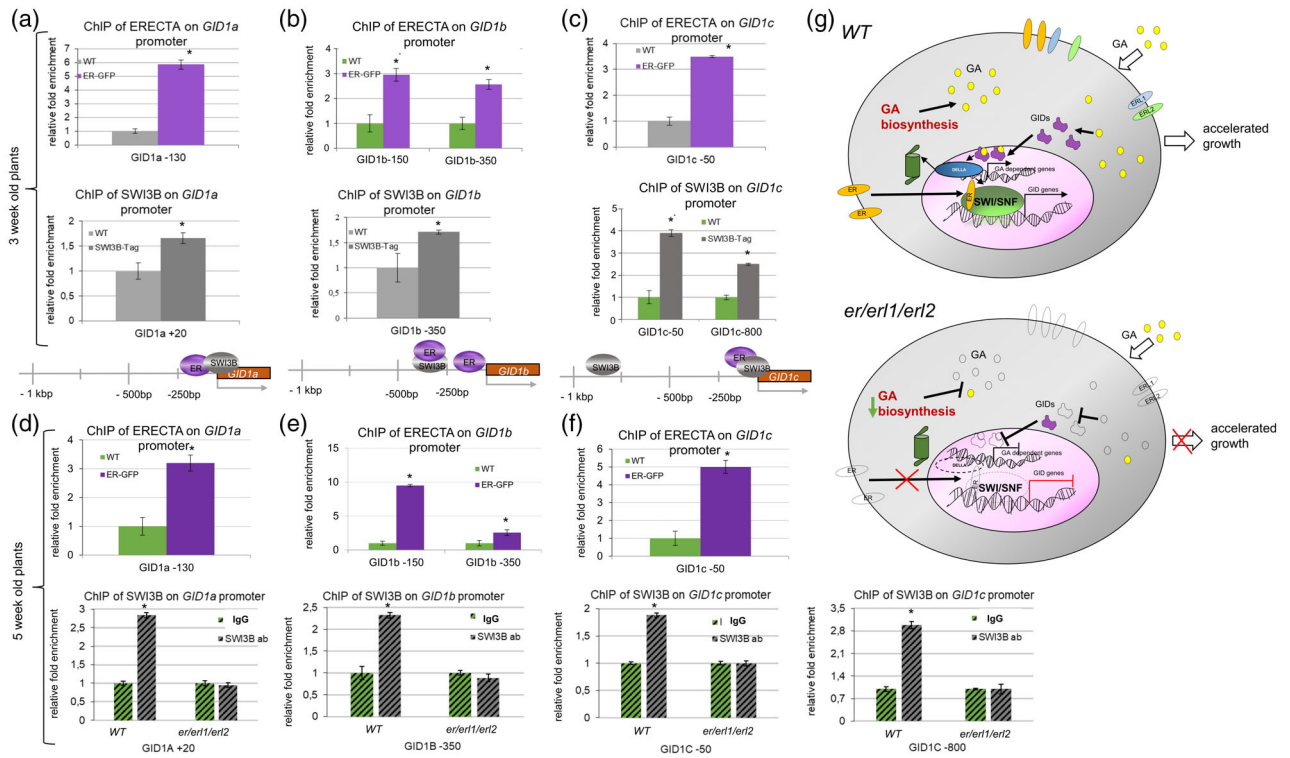
Figure 6. ERf proteins enter the nucleus where ERECTA protein binds the GID1 promoters similarly to the SWI3B subunit of SWI/SNF CRC.

(a) ERECTA protein binds to promoter regions of the *GID1a* gene in a region targeted by the SWI/SNF complex in 3-week-old plants (error bars refer to SD, *P* < 0.05, Student's *t*-test, three biological and technical replicates were performed). ChIP, chromatin immunoprecipitation; WT, wild type.

(b) ERECTA and SWI3B core subunit of SWI/SNF CRCs target promoter regions of *GID1b* gene in 3-week-old plants (error bars refer to SD, *P* < 0.05, Student's *t*-test, three biological and technical replicates were performed).

(c) SWI3B binds to the promoter region of the *GID1c* gene in two different regions. One of them is targeted by ERECTA protein in 3-week-old plants.

(d) ERECTA protein binds to promoter regions of the *GID1a* gene in a region targeted by the SWI/SNF complex in 5-week-old plants (error bars refer to SD, *P* < 0.05, Student's *t*-test, three biological and technical replicates were performed).

(e) ERECTA targets promoter region of *GID1b* gene in 5-week-old plants (error bars refer to SD, *P* < 0.05, Student's *t*-test, three biological and technical replicates were performed).

(f) ERECTA binds to the promoter region of the *GID1c* gene in 3-week-old plants. Bottom panel in (d–f): the binding of native SWI3B protein to its target sites in *GID1a-c* promoter regions is abolished in 5-week-old *er/erl1/erl2* triple mutant plants.

(g) Model describing the non-canonical nuclear function of ERf proteins in the gibberellin (GA) signaling pathway.

around −150 bp and −350 bp from the TSS in the *GID1b* promoter, SWI3B was localized only −350 bp upstream to TSS (Figure 6b). ER and SWI3B were similarly cross-linked to the −100 bp region of the *GID1c* promoter, but SWI3B was also mapped further upstream to −800 bp (Figure 6c).

Inspection of ER and SWI3B binding to the *GID1a-c* promoter regions in 5-week-old WT, ER-GFP, and the *er/erl1/erl2* mutant demonstrated that ER binds the same *GID1* promoter regions as in the case of 3-week-old plants (Figure 6d–f). The SWI3B binding to the promoter of *GID1* genes was abolished by the inactivation of ERf proteins in *er/erl1/erl2* plants. The inactivation of *ER*, *ERL1*, or *ERL2* did not affect the binding of the SWI3B to *GID1a-c* promoter regions in single *er105*, *erl1*, and *erl2* mutant lines (Figure S16). Our study provides evidence that the three ERf proteins have redundant functions regarding proper SWI3B recruitment as only the simultaneous absence of all ERf proteins abolished SWI3B binding to the *GID1a-c* promoters.

Of note, we found a similar binding of HER2 (EGFR-family) receptor and BAF155 subunit of SWI/SNF CRCs to the promoter regions of human *BRCA1* and *FBP1* genes (Figure S17), indicating that the phenomenon observed for ER may be a general mechanism controlling gene expression that is maintained between kingdoms.

DISCUSSION

Genetic inactivation of ERf LRR-RLK family members results in various defects in *Arabidopsis* growth and development. While it is well established that ERf proteins play distinct roles in the mediation of epidermal patterning, stomatal development, meristem size, inflorescence architecture, and hormonal signaling, the exact mechanisms underlying the regulatory functions of ERf proteins in these processes are largely unknown (e.g., Chen et al., 2013; Chen & Shpak, 2014; Kosentka et al., 2019; Qi et al., 2004; Van Zanten et al., 2010).

Here we showed that the inactivation of *Arabidopsis* ERf proteins has a broad effect on various important processes, including hormonal signaling, and suggest that these sum responses underlie the severe developmental defects exhibited by the *er/erl1/erl2* mutant. We demonstrate that parallel inactivation of all ERf proteins results in severe defect of the GA signaling pathway as evidenced by the impairment of GA perception and GA biosynthesis. When taken together, these findings, alongside the identification of NLS and NES sequences in ERf proteins and our demonstration of their translocation into the nucleus, suggest a not yet recognized, non-canonical function of ERf proteins (Figure 6g).

Our study also reveals an analogy of this system to the previously described XA21 LRR immune receptor in rice (Park & Ronald, 2012) and to the non-canonical signaling mode of the human EGFR family (Lee, Wang, & Hung, 2015). Although it should be stressed that these two classes of plant and animal epidermal receptors carry completely unrelated sequences from one another and from the system we describe here (Table S3), suggesting that the translocation of the membrane receptors to the nucleus may be a general paradigm maintained between plant and animal kingdoms. In addition to their canonical membrane receptor functions, holoreceptor and truncated forms of EGFRs are imported into nuclei via ER-mediated retrograde transport, although some of them lack known NLSs (Chen & Hung, 2015).

In the nucleus, the EGFR receptors can bind to DNA, interact with various transcription factors. Thereby, nuclear forms of EGFRs are implicated in the control of cell proliferation, DNA replication and repair, and transcription (Chen & Hung, 2015), so their functions extend far beyond the influence of epidermal patterning.

We found here that the *Arabidopsis* ERECTA LRR-RLK receptor translocates from the plasma membrane into the nucleus. Both the intact and the N-terminally truncated forms of ERECTA were detectable in the nucleus. A truncated ERECTA carrying only the kinase domain localizes exclusively in the nucleus and partially complements the leaf developmental defects caused by the *er-105* mutation implying a ligand-independent non-canonical signaling function of the ERECTA kinase domain.

Furthermore, our data show that the ERf proteins interact through their kinase domains with the SWI3B, and ER can phosphorylate the SWI3B core subunit of the SWI/SNF CRC. SWI/SNF plays a pivotal role in the interface of hormonal signaling pathways in both humans and plants (Sarnowska et al., 2016). Moreover, we show that analogously to the ER protein, the HER2 member of the EGFR family directly interacts with the BAF155 subunit of human SWI/SNF and co-localizes with BAF155 on some gene promoters providing evidence that such a system is likely maintained between kingdoms.

Parallel inactivation of all ERf proteins results in alterations of genome-wide nucleosomal chromatin structure and altered transcriptional activity of a large number of genes. The binding of SWI3B to its target regions in the *GID1a-c* promoters is retained in *er-105*, *erl1*, and *erl2* single mutant lines. By contrast, the *er/erl1/erl2* mutant plants exhibited a reduction in phosphorylation and SWI3B protein level and abolished proper SWI3B binding to *GID1* promoter regions together with the decreased expression of *GID1a-c* genes. These results indicate a strong and direct effect of the ERf signaling pathway and ER phosphorylation of SWI3B on SWI/SNF-dependent chromatin remodeling. Moreover, the observed interdependence between the ERf signaling and SWI3B supports the transcriptional alterations exhibited by *er/erl1/erl2* plants.

Our understanding of the function of SWI3B in GA signaling was further extended by the identification of interdependence between RGA DELLA protein and the SWI3B subunit of SWI/SNF CRCs. We have shown that accumulation of DELLA in WT and *ga1-3* *Arabidopsis* plants leads to a decrease of SWI3B levels. This finding is in line with the well documented function of DELLA proteins in transcription factor sequestration (for review see Phokas & Coates, 2021) and previously published data indicating DELLA-dependent sequestration and protein level control (degradation) for the PICKLE chromatin remodeler (Zhang et al., 2014). We found that similarly as *Arabidopsis* plants with impaired/inactivated SWI/SNF subunits (BRM and SWI3C), *er/erl1/erl2* plants exhibiting reduced levels of SWI3B protein do not accumulate DELLA. All the mutants are characterized by a decreased level of bioactive GA; therefore, it would be anticipated that these plants accumulate DELLA proteins. The downregulation of DELLA genes transcripts shown by us in *er/erl1/erl2* plants and previously observed for the *swi3c* decrease of *RGA*, *RGL1*, *RGL3*, and *GAI* expression (Sarnowska et al., 2013), likely explain the lack of accumulation of DELLA proteins in these plants and indicate the possible existence of multiple levels of DELLA expression control or feedback loop, thus extend the picture of the DELLA regulation system. On the other hand, the DELLA protein abundance is controlled also at the protein level. Hence, we cannot exclude the possibility that there exist another mechanism and/or feedback loop related to the abundance of SWI/SNF CRCs and DELLA proteins. However, substantiation of this study would require additional study.

Collectively our findings were that plant ERf proteins play an important, non-canonical nuclear function. In this they bind directly to chromatin, control the SWI3B phosphorylation, and lead to proper recruitment of SWI3B-containing SWI/SNF CRCs. Together these are associated in controlling regulatory processes, including interdependence between hormonal pathways (Sarnowska et al., 2016), thus our findings may be a general paradigm for other classes of plant and mammalian membrane receptor

kinases. Given the broad effect of ERf proteins, SWI/SNF CRCs, and DELLA proteins on the *Arabidopsis* growth, development, and other important processes, our study represents an important indication for the future possibilities to explore the interplay between ERf signaling, DELLA repressors, and SWI/SNF-dependent chromatin remodeling.

EXPERIMENTAL PROCEDURES

Plant material and growth conditions

Arabidopsis thaliana ecotype Columbia was used as WT in all experiments. The following Arabidopsis mutants were used for analysis: *er-105*, *er-105/swi3b-3* (Sáez et al., 2008), and *er/erl1/erl2* plants (Shpak et al., 2004), and *erf* lines in various combinations (Torii et al., 1996), the 35S::GFP Arabidopsis line has been obtained from NASC (N67775). Seeds were sown on soil or plated on half Murashige and Skoog medium (Sigma-Aldrich) containing 0.5% sucrose and 0.8% agar. Plants were grown under long day conditions (12 h day/12 h night or 16 h day/8 h night). For GA response tests, plants were sprayed twice a week with 100 μM GA$_{4 + 7}$ or water (control) for a fast response the 2 h of GA$_{4 + 7}$ treatment was performed.

Construction of transgenic lines

Genomic sequences of *ERECTA*, cDNAs of *ERECTA* kinase domain and truncated ERECTA lacking kinase domain (ERΔK) were cloned into binary vector p35S::GW::GFP (F. Turck, Max-Planck-Institut für Züchtungsforschung, in the case of ERECTA), and into pEarley Gate 101 (in the case of the ER kinase domain and ΔKDER; (Earley et al., 2006)). Plants were transformed using *Agrobacterium tumefaciens* GV3101 (pMP90) by floral-dip method (Davis et al., 2009). The STOP codon of the *SWI3B* genomic sequence was replaced with HIS-STREP-HA using the recombineering method (Bitrián et al., 2011), moved into pCB1 vector (Heidstra et al., 2004), and transformed into *swi3b-2* Arabidopsis mutant line.

RNA extraction and quantitative real-time PCR analysis

Total RNA was isolated from adult (5-week-old) plants using an RNeasy plant kit (Qiagen), treated with a TURBO DNA-free kit (Ambion). Total RNA (2.5 μg) was reverse transcribed using a first-strand cDNA synthesis kit (Roche). Quantitative real-time PCR assays were performed with SYBR Green Master mix (Bio-Rad) and specific primers for PCR amplification. Housekeeping genes *PP2A* and *UBQ5* (AT1G13320 and AT3G62250, respectively) were used as controls. The relative transcript level of each gene was determined by the $2^{-\Delta\Delta Ct}$ method (Schmittgen & Livak, 2008). Each experiment was performed using at least three independent biological replicates. Quantitative real-time PCR primers are listed in Data S3, primers for DELLA encoding genes were published in Sarnowska et al. (2013).

Transcript profiling and gene ontology analysis

RNA was isolated from adult (5-week-old) WT and *er/erl1/erl2* plants using a Plant RNeasy kit (Qiagen) according to the manufacturer's protocol. Transcriptomes were analyzed using 150 ng of total RNA as starting material. Targets were prepared with a cDNA synthesis kit followed by biotin labeling with the IVT labeling kit (GeneChip 39IVT Express; Affymetrix) and hybridized to the ATH1 gene chip for 16 h as recommended by the supplier. The raw data were analyzed using GenespringGX according to the manual

(guided workflow). GO-TermFinder was used for GO analyses of selected groups of genes (Boyle et al., 2004).

Nuclear fractionation

Nuclei were isolated from 2 g of leaves of 3-week-old *Arabidopsis* seedlings according to the method previously described by Gaudino and Pikaard (1997). Subsequent nuclear fractionation was performed using the high-salt method, with modifications (Sarnowski et al., 2002).

Anti-H3 (ab1791; Abcam) and anti-H + ATPase (AS07260; Agrisera) antibodies were used for quality controls of nuclei purity.

Protein interaction study, confocal imaging, subcellular localization, BFA and leptomycin B treatment, and 4′,6-diamidino-2-phenylinodole staining

Protein interaction was analyzed by performing the immunoprecipitation of ER-GFP or KDER-YFP-HA from nuclei from 4 g of *Arabidopsis* plants (Saleh et al., 2008). The nuclear extracts were incubated with 25 μl of GFP Magnetic Trap beads (Chromotek) according to the manufacturer's instructions. The presence of SWI3B protein was determined by Western blot analysis using anti-SWI3B antibody (Sarnowski et al., 2002).

The interaction between human proteins was analyzed by immunoprecipitation of HER2 and BAF155 from viscolase-treated nuclear extracts prepared, according to (Jancewicz et al., 2021). The presence of HER2 and BAF155 was determined by Western blot analysis using anti-HER2 (CST, 12760) and anti-BAF155 (CST, 11956) antibodies.

To obtain YFN-ERL1, YFC-ERL1, YFC-ERL2, and YFC-KDER fusions for BiFC (Hu et al., 2002) analysis, cDNAs encoding ERL1 and ERL2 proteins and ERECTA, ERL1, and ERL2 C-terminal kinase domains were PCR amplified and cloned into the binary vectors pYFN43 or pYFC43 (Belda-Palazón et al., 2012). The *in vivo* interactions between proteins were detected by BiFC using Leica TCS SP2 AOBS, a laser scanning confocal microscope (Leica Microsystems).

Tobacco (*N. benthamiana*) epidermal cells were infiltrated using *A. tumefaciens* GV3101 (pMP90) carrying plasmids encoding ERL1, ERL2, or KDER fusions and the p19 helper vector and analyzed by confocal microscopy 3 days later. YFN-RFP and YFC-RFP fusions were used to detect transformed cells in the BiFC assays (Sarnowska et al., 2013); at least five nuclei were analyzed in three separate experiments.

The vesicle trafficking inhibitor BFA (Sigma-Aldrich) was used at the 25 μM concentration at the following time points 40, 90, and 120 min. The NES-dependent nuclear export inhibitor leptomycin B was used at the 200 nM concentration 4 h before microscopy observation. Nuclei were stained with 4′,6-diamidino-2-phenylinodole (DAPI) at the 1 μg ml^{-1} concentration for 30 min. The observation was carried out on the root tip of about 2-week-old plants incubated directly before in half Murashige and Skoog medium alone or with the addition of proper compound (BFA or leptomycin B, respectively). Every time 30 min before the end of incubation, DAPI was added.

Chromatin immunoprecipitation

ChIP experiments were performed as described previously (Sacharowski et al., 2015) on 3- or 5-week-old WT, ER-GFP, SWI3B-His-Strep-HA, and *er/erl1/erl2* plants cross-linked under vacuum using formaldehyde (final concentration: 1%) and *bis*-(sulfosuccinimidyl) glutarate (final concentration: 1 mM). For ER-GFP, chromatin

immunoprecipitation was performed with GFP-Trap M (Chromotek). For SWI3B ChIP experiments, NiNTA Agarose (Qiagen) or, in the case of anti-SWI3B antibody, the magnetic protein A and G dynabeads (Dynal) were used. ChIP enrichment was determined using quantitative PCR, and relative fold change was calculated using the $2^{-\Delta\Delta Ct}$ method (Schmittgen & Livak, 2008). The TA3 retrotransposon was used as negative control (Pastore et al., 2011). Primers used in ChIP experiments are listed in Data S3.

GA analysis

About 200 mg of frozen materials from 5-week-old plants were used to extract and purify the GA as described in Plackett et al. (2012) with minor modifications. GA was quantified using tandem mass spectrometry (MS/MS) analysis using 4000 Triple Quad (AB Sciex Germany GmbH) in multiple reaction monitoring scan with electrospray ionization as described in Salem et al. (2016). The MS attached to the UPLC system (e.g., Waters Acquity UPLC system; Waters) separation was achieved on a reversed phase C18-column (100 mm × 2.1 mm 1.8 μm).

In vivo phosphorylation analysis and *in vitro* kinase assay

SWI3B-6xHis was overexpressed and purified, according to Sarnowski et al. (2002). The KDER (pDEST-6xHis-MBP vector) was purified using tandem purification using MBP and Ni-NTA resins. *In vitro* kinase assay was performed according to the method described by Allen et al. (2007). Phosphorylation was detected by Western blot analysis using an anti-thiophosphate ester antibody (ab92570; Abcam) and by the MS/MS analysis.

In vivo phosphorylation analysis was performed using a 2D Western blot assay on nuclear extracts from 5-week-old WT and *er/erl1/erl2* plants (Saleh et al., 2008). For IEF, nuclear proteins were prepared according to Kubala et al. (2015). The IEF was performed on the 7 cm length gel strips with immobilized pH gradients 3–10 and 3–6 (Bio-Rad). After IEF, the equilibration of immobilized pH gradient was performed according to Wojtyla et al. (2013). The SWI3B protein was detected by Western blotting using an anti-SWI3B antibody (Sarnowski et al., 2002). The *in vivo* phosphorylation was identified based on the changes of SWI3B isoelectric point (*pI*) (Mayer et al., 2015).

ACCESSION NUMBERS

ERECTA (AT2G26330), ERL1 (AT5G62230), ERL2 (AT5G07180), SWI3B (AT2G33610), SWI3C (AT1G21700), BRM (AT2G46020), GID1a (AT3G05120), GID1b (AT3G63010), GID1c (AT5G27320), RGA (AT2G01570), GAI (AT1G14920), RGL1 (AT1G66350), RGL2 (AT3G03450), RGL3 (AT5G17490).

AUTHOR CONTRIBUTIONS

TJS, ES, and SJD planned experiments and wrote the manuscript. SK and PC participated in the planning of some experiments. TJS, ES, SK, PC, SS, SA, BH, JAS, and ARF analyzed the data. ES, PC, SS, SK, PO, JS, MZ, JMS, RD, AM, MS, BH, MC, KN, ATR, EB, RF, AS, MAD, SA, MRH, and TJS performed experiments. All authors read, edited, and approved the final manuscript.

CONFLICT OF INTEREST STATEMENT

The authors declare that they have no competing interests.

DATA AVAILABILITY STATEMENT

Microarray and MNase-seq data are available in the ArrayExpress database (www.ebi.ac.uk/arrayexpress) under E-MTAB-5595 and E-MTAB-5830 accession numbers, respectively.

SUPPORTING INFORMATION

Additional Supporting Information may be found in the online version of this article.

Figure S1. Comparative analysis of genes with altered expression in *er/erl1/erl2* and *ga1-3* mutants.

Figure S2. *er/erl1/erl2* mutant displays severely impaired response to exogenous GA treatment and slightly enhance *ga1-3* phenotypic traits.

Figure S3. *er/erl1/erl2* plants exhibit deficiency in gibberellin intermediates, lack of GAI DELLA protein accumulation and decreased expression of genes encoding DELLA proteins.

Figure S4. 35S::ERECTA-GFP construct complements the *er-105* mutation.

Figure S5. ERECTA protein is detected in various cell compartments including endosomes and accumulate in the nuclei periphery after BFA treatment.

Figure S6. ERL1 and ERL2 proteins carry defined NLS in their kinase domains.

Figure S7. The kinase domain of ERECTA (KDER) has ability to complement the *er-105* leaf phenotypic traits.

Figure S8. ERECTA protein enters to the nucleus and localizes in various sub-nuclear fractions.

Figure S9. Negative controls for bimolecular fluorescence complementation assay.

Figure S10. Human SWI3-type BAF155 co-precipitates with HER2 EGFR family membrane receptor from human cells nuclei.

Figure S11. *er/elr1/erl2* mutant plants show affected chromatin organization demonstrated as altered chromocenters number.

Figure S12. ERf proteins inactivation has a severe impact on genome-wide nucleosome positioning.

Figure S13. Kinase domain of ERECTA phosphorylates SWI3B protein.

Figure S14. GA-deficient mutant lines with inactivated subunits of SWI/SNF complexes do not accumulate RGA and GAI DELLA proteins.

Figure S15. Negative controls for bimolecular fluorescence complementation assay (SWI3B-DELLA interactions).

Figure S16. Proper SWI3B binding to GID1a-c promoter regions is abolished in the *er/erl1/erl2* whereas occurs in single *er-105*, *erl1* or *erl2* mutant lines.

Figure. S17. Human SWI3-type BAF155 targets together with HER2 EGFR family membrane receptor *FBP1* and *BRCA1* genes *loci*.

Table S1. Genes classified to "Response to Gibberellin" GO term and showing downregulated expression level in the *er/erl1/erl2* mutant transcript profiling.

Table S2. Genes with upregulated expression in *er/erl1/erl2* mutant plants classified to GO-terms of leaf epidermal and stomatal cell differentiation.

Table S3. Functional analogies between Arabidopsis ERf proteins and the human EGFR membrane receptors.

Appendix S1. Method S1 chromatin immunoprecipitation from human cell line. Chromatin from the SKBR-3 human cell line was immunoprecipitated according to (Komata et al., 2014; Jancewicz et al., 2021). Recovered chromatin was incubated O/N at 4°C with the following antibodies: anti-BAF155 (CST, 11956), antiHER2 (CST, 12760), and normal rabbit IgG (CST, 2729, mock control). Results were calculated based on the $2^{-\Delta\Delta Ct}$ (Schmittgen & Livak, 2008). Relative fold enrichment of the analyzed sample represents the fold change with reference to IgG (mock) sample. A set of primers used for ChIP-qPCR analysis is listed in Supplementary Dataset 3.

Method S2. MNase mapping of genome-wide nucleosome positioning and MNase-qPCR. Nuclear extraction, MNase treatment, subsequent NGS analyses and confirmatory MNase-qPCR were performed according to (Sacharowski et al., 2015) on 5-week-old plant material.

Movie S1. ERECTA protein undergoes endocytosis.

Movie S2. ERECTA protein undergoes endocytosis.

Data S1. Comparative analysis of transcript profiling and MNase-seq data.

Data S2. Comparison of ER, ERL1, and ERL2 protein sequences with highlighted important domains including NLS.

Data S3. Primers used in this work.

REFERENCES

Allen, J.J., Li, M., Brinkworth, C.S., Paulson, J.L., Wang, D., Hübner, A. et al. (2007) A semisynthetic epitope for kinase substrates. *Nature Methods*, **46**(4), 511–516.

Archacki, R., Buszewicz, D., Sarnowski, T.J., Sarnowska, E., Rolicka, A.T., Tohge, T. et al. (2013) BRAHMA ATPase of the SWI/SNF chromatin remodeling complex acts as a positive regulator of gibberellin-mediated responses in Arabidopsis. *PLoS One*, **8**, e58588.

Archacki, R., Yatusevich, R., Buszewicz, D., Krzyczmonik, K., Patryn, J., Iwanicka-Nowicka, R. et al. (2016) Arabidopsis SWI/SNF chromatin remodeling complex binds both promoters and terminators to regulate gene expression. *Nucleic Acids Research*, **45**, 3116–3129.

Belda-Palazón, B., Ruiz, L., Martí, E., Tárraga, S., Tiburcio, A.F., Culiáñez, F. et al. (2012) Aminopropyltransferases involved in polyamine biosynthesis localize preferentially in the nucleus of plant cells. *PLoS One*, **7**, e46907.

Bitrián, M., Roodbarkelari, F., Horváth, M. & Koncz, C. (2011) BAC-recombineering for studying plant gene regulation: developmental

control and cellular localization of SnRK1 kinase subunits. *The Plant Journal*, **65**, 829–842.

Boyle, E.I., Weng, S., Gollub, J., Jin, H., Botstein, D., Cherry, J.M. et al. (2004) GO::TermFinder - open source software for accessing gene ontology information and finding significantly enriched gene ontology terms associated with a list of genes. *Bioinformatics*, **20**, 3710–3715.

Cai, H., Huang, Y., Chen, F., Liu, L., Chai, M., Zhang, M. et al. (2021) ERECTA signaling regulates plant immune responses via chromatin-mediated promotion of WRKY33 binding to target genes. *The New Phytologist*, **230**, 737–756.

Cai, H., Zhao, L., Wang, L., Zhang, M., Su, Z., Cheng, Y. et al. (2017) ERECTA signaling controls Arabidopsis inflorescence architecture through chromatin-mediated activation of PRE1 expression. *The New Phytologist*, **214**, 1579–1596.

Cao, D., Cheng, H., Wu, W., Soo, H.M. & Peng, J. (2006) Gibberellin mobilizes distinct DELLA-dependent transcriptomes to regulate seed germination and floral development in Arabidopsis. *Plant Physiology*, **142**, 509–525.

Chen, M.K. & Hung, M.C. (2015) Proteolytic cleavage, trafficking, and functions of nuclear receptor tyrosine kinases. *The FEBS Journal*, **282**, 3693–3721.

Chen, M.K. & Shpak, E.D. (2014) ERECTA family genes regulate development of cotyledons during embryogenesis. *FEBS Letters*, **588**, 3912–3917.

Chen, M.-K., Wilson, R.L., Palme, K., Ditengou, F.A. & Shpak, E.D. (2013) ERECTA family genes regulate auxin transport in the shoot apical meristem and forming leaf primordia. *Plant Physiology*, **162**, 1978–1991.

Davis, A.M., Hall, A., Millar, A.J., Darrah, C. & Davis, S.J. (2009) Protocol: streamlined sub-protocols for floral-dip transformation and selection of transformants in Arabidopsis thaliana. *Plant Methods*, **5**, 3.

Du, J., Jiang, H., Sun, X. et al. (2018) Auxin and gibberellins are required for the receptor-like kinase ERECTA regulated hypocotyl elongation in shade avoidance in Arabidopsis. *Frontiers in Plant Science*, **9**, 124.

Earley, K.W., Haag, J.R., Pontes, O., Opper, K., Juehne, T., Song, K. et al. (2006) Gateway-compatible vectors for plant functional genomics and proteomics. *The Plant Journal*, **45**(4), 616–629.

Gaudino, R.J. & Pikaard, C.S. (1997) Cytokinin induction of RNA polymerase I transcription in Arabidopsis thaliana. *The Journal of Biological Chemistry*, **272**, 6799–6804.

Giri, D.K., Ali-Seyed, M., Li, L.-Y., Lee, D.-F., Ling, P., Bartholomeusz, G. et al. (2005) Endosomal transport of ErbB-2: mechanism for nuclear entry of the cell surface receptor. *Molecular and Cellular Biology*, **25**, 11005–11018.

Griffiths, J., Murase, K., Rieu, I., Zentella, R., Zhang, Z.L., Powers, S.J. et al. (2006) Genetic characterization and functional analysis of the GID1 gibberellin receptors in Arabidopsis. *Plant Cell*, **18**, 3399–3414.

Haasen, D., Köhler, C., Neuhaus, G. & Merkle, T. (2002) Nuclear export of proteins in plants: AtXPO1 is the export receptor for leucine-rich nuclear export signals in Arabidopsis thaliana. *The Plant Journal*, **20**, 695–705.

Heidstra, R., Welch, D. & Scheres, B. (2004) Mosaic analyses using marked activation and deletion clones dissect Arabidopsis SCARECROW action in asymmetric cell division. *Genes & Development*, **18**, 1964–1969.

Ho, C.M.K., Paciorek, T., Abrash, E. & Bergmann, D.C. (2016) Modulators of stomatal lineage signal transduction Alter membrane contact sites and reveal specialization among ERECTA kinases. *Developmental Cell*, **38**, 345–357.

Hu, C.D., Chinenov, Y. & Kerppola, T.K. (2002) Visualization of interactions among bZIP and Rel family proteins in living cells using bimolecular fluorescence complementation. *Molecular Cell*, **9**, 789–798.

Hung, L.Y., Tseng, J.T., Lee, Y.C., Xia, W., Wang, Y.N., Wu, M.L. et al. (2008) Nuclear epidermal growth factor receptor (EGFR) interacts with signal transducer and activator of transcription 5 (STAT5) in activating Aurora-a gene expression. *Nucleic Acids Research*, **36**, 4337–4351.

Jancewicz, I., Szarkowska, J., Konopinski, R., Stachowiak, M., Swiatek, M., Blachnio, K. et al. (2021) PD-L1 overexpression, SWI/SNF complex deregulation, and profound transcriptomic changes characterize cancer-dependent exhaustion of persistently activated CD4+ T cells. *Cancers*, **13**, 4148.

Komata, M., **Katou, Y.**, **Tanaka, H.**, **Nakato, R.**, **Shirahige, K.** & **Bando, M.** (2014) Chromatin immunoprecipitation protocol for mammalian cells. *Methods in Molecular Biology*, **1164**, 33–38.

Kosentka, P.Z., **Overholt, A.**, **Maradiaga, R.**, **Mitoubsi, O.** & **Shpak, E.D.** (2019) EPFL signals in the boundary region of the SAM restrict its size and promote leaf initiation. *Plant Physiology*, **179**, 265–279.

Kosentka, P.Z., **Zhang, L.**, **Simon, Y.A.**, **Satpathy, B.**, **Maradiaga, R.**, **Mitoubsi, O.** *et al.* (2017) Identification of critical functional residues of receptor-like kinase ERECTA. *Journal of Experimental Botany*, **68**, 1507–1518.

Kosugi, S., **Hasebe, M.**, **Tomita, M.** & **Yanagawa, H.** (2009) Systematic identification of cell cycle-dependent yeast nucleocytoplasmic shuttling proteins by prediction of composite motifs. *Proceedings of the National Academy of Sciences of the United States of America*, **106**, 10171–10176.

Kubala, S., **Garnczarska, M.**, **Wojtyla, Ł.**, **Clippe, A.**, **Kosmala, A.**, **Zmieńko, A.** *et al.* (2015) Deciphering priming-induced improvement of rapeseed (Brassica napus L.) germination through an integrated transcriptomic and proteomic approach. *Plant Science*, **231**, 94–113.

La Cour, T., **Kiemer, L.**, **Mølgaard, A.**, **Gupta, R.**, **Skriver, K.** & **Brunak, S.** (2004) Analysis and prediction of leucine-rich nuclear export signals. *Protein Engineering, Design & Selection*, **17**, 527–536.

La Rosa, N.M., **Pfeiffer, A.**, **Hill, K.**, **Locascio, A.**, **Bhalerao, R.P.**, **Miskolczi, P.** *et al.* (2015) Genome wide binding site analysis reveals transcriptional Coactivation of Cytokinin-responsive genes by DELLA proteins. *PLoS Genetics*, **11**, e1005337.

Lee, H.-H., **Wang, Y.-N.** & **Hung, M.-C.** (2015) Non-canonical signaling mode of the epidermal growth factor receptor family. *American Journal of Cancer Research*, **5**, 2944–2958.

Lee, J.S., **Hnilova, M.**, **Maes, M.**, **Lin, Y.-C.L.**, **Putarjunan, A.**, **Han, S.-K.** *et al.* (2015) Competitive binding of antagonistic peptides fine-tunes stomatal patterning. *Nature*, **522**, 439–443.

Lee, J.S., **Kuroha, T.**, **Hnilova, M.**, **Khatayevich, D.**, **Kanaoka, M.M.**, **Mcabee, J.M.** *et al.* (2012) Direct interaction of ligand-receptor pairs specifying stomatal patterning. *Genes & Development*, **26**, 126–136.

Li, C., **Gu, L.**, **Gao, L.**, **Chen, C.**, **Wei, C.Q.**, **Qiu, Q.** *et al.* (2016) Concerted genomic targeting of H3K27 demethylase REF6 and chromatin-remodeling ATPase BRM in Arabidopsis. *Nature Genetics*, **48**, 687–693.

Mayer, K., **Albrecht, S.** & **Schaller, A.** (2015) Targeted analysis of protein phosphorylation by 2D electrophoresis. *Methods in Molecular Biology*, **1306**, 167–176.

Miller, S.G., **Carnell, L.** & **Moore, H.P.H.** (1992) Post-Golgi membrane traffic: Brefeldin a inhibits export from distal Golgi compartments to the cell surface but not recycling. *The Journal of Cell Biology*, **118**, 267–283.

Park, C.J. & **Ronald, P.C.** (2012) Cleavage and nuclear localization of the rice XA21 immune receptor. *Nature Communications*, **3**, 920.

Pastore, J.J., **Limpuangthip, A.**, **Yamaguchi, N.**, **Wu, M.F.**, **Sang, Y.**, **Han, S.K.** *et al.* (2011) LATE MERISTEM IDENTITY2 acts together with LEAFY to activate APETALA1. *Development*, **138**, 3189–3198.

Phokas, A. & **Coates, J.C.** (2021) Evolution of DELLA function and signaling in land plants. *Evolution & Development*, **23**, 137–154.

Plackett, A.R.G., **Powers, S.J.**, **Fernandez-Garcia, N.**, **Urbanova, T.**, **Takebayashi, Y.**, **Seo, M.** *et al.* (2012) Analysis of the developmental roles of the Arabidopsis gibberellin 20-oxidases demonstrates that GA20ox1, −2, and -3 are the dominant paralogs. *Plant Cell*, **24**, 941–960.

Qi, Y., **Sun, Y.**, **Xu, L.**, **Xu, Y.** & **Huang, H.** (2004) ERECTA is required for protection against heat-stress in the AS1/AS2 pathway to regulate adaxial-abaxial leaf polarity in Arabidopsis. *Planta*, **219**, 270–276.

Ragni, L., **Nieminen, K.**, **Pacheco-Villalobos, D.**, **Sibout, R.**, **Schwechheimer, C.** & **Hardtke, C.S.** (2011) Mobile gibberellin directly stimulates Arabidopsis hypocotyl xylem expansion. *Plant Cell*, **23**, 1322–1336.

Sacharowski, S.P., **Gratkowska, D.M.**, **Sarnowska, E.A.**, **Kondrak, P.**, **Jancewicz, I.**, **Porri, A.** *et al.* (2015) SWP73 subunits of arabidopsis SWI/SNF chromatin remodeling complexes play distinct roles in leaf and flower development. *Plant Cell*, **27**, 1889–1906.

Sáez, A., **Rodrigues, A.**, **Santiago, J.**, **Rubio, S.** & **Rodriguez, P.L.** (2008) HAB1-SWI3B interaction reveals a link between abscisic acid signaling and putative SWI/SNF chromatin-remodeling complexes in Arabidopsis. *Plant Cell*, **20**, 2972–2988.

Saleh, A., **Alvarez-Venegas, R.** & **Avramova, Z.** (2008) An efficient chromatin immunoprecipitation (ChIP) protocol for studying histone modifications in Arabidopsis plants. *Nature Protocols*, **3**, 1018–1025.

Salem, M.A., **Jüppner, J.**, **Bajdzienko, K.** & **Giavalisco, P.** (2016) Protocol: a fast, comprehensive and reproducible one-step extraction method for the rapid preparation of polar and semi-polar metabolites, lipids, proteins, starch and cell wall polymers from a single sample. *Plant Methods*, **121**(12), 1–15.

Sarnowska, E., **Gratkowska, D.M.**, **Sacharowski, S.P.**, **Cwiek, P.**, **Tohge, T.**, **Fernie, A.R.** *et al.* (2016) The role of SWI/SNF chromatin remodeling complexes in hormone crosstalk. *Trends in Plant Science*, **21**, 594–608.

Sarnowska, E.A., **Rolicka, A.T.**, **Bucior, E.**, **Cwiek, P.**, **Tohge, T.**, **Fernie, A.R.** *et al.* (2013) DELLA-interacting SWI3C Core subunit of switch/sucrose nonfermenting chromatin remodeling complex modulates gibberellin responses and hormonal cross talk in Arabidopsis. *Plant Physiology*, **163**, 305–317.

Sarnowski, T.J., **Swiezewski, S.**, **Pawlikowska, K.**, **Kaczanowski, S.** & **Jerzmanowski, A.** (2002) AtSWI3B, an Arabidopsis homolog of SWI3, a core subunit of yeast SWI/Snf chromatin remodeling complex, interacts with FCA, a regulator of flowering time. *Nucleic Acids Research*, **30**, 3412–3421.

Schmittgen, T.D. & **Livak, K.J.** (2008) Analyzing real-time PCR data by the comparative CT method. *Nature Protocols*, **3**, 1101–1108.

Shpak, E.D. (2003) Dominant-negative receptor uncovers redundancy in the Arabidopsis ERECTA leucine-rich repeat receptor-like kinase signaling pathway that regulates organ shape. *Plant Cell Online*, **15**, 1095–1110.

Shpak, E.D. (2013) Diverse roles of ERECTA family genes in plant development. *Journal of Integrative Plant Biology*, **55**, 1238–1250.

Shpak, E.D., **Berthiaume, C.T.**, **Hill, E.J.** & **Torii, K.U.** (2004) Synergistic interaction of three ERECTA-family receptor-like kinases controls Arabidopsis organ growth and flower development by promoting cell proliferation. *Development*, **131**, 1491–1501.

Shpak, E.D., **McAbee, J.M.**, **Pillitteri, L.J.** & **Torii, K.U.** (2005) Stomatal patterning and differentiation by synergistic interactions of receptor kinases. *Science*, **309**, 290–293.

Torii, K.U., **Mitsukawa, N.**, **Oosumi, T.**, **Matsuura, Y.**, **Yokoyama, R.**, **Whittier, R.F.** *et al.* (1996) The Arabidopsis ERECTA gene encodes a putative receptor protein kinase with extracellular leucine-rich repeats. *Plant Cell*, **8**, 735–746.

Torii, K.U., **Pillitteri, L.J.**, **Sloan, D.B.** & **Bogenschutz, N.L.** (2007) Termination of asymmetric cell division and differentiation of stomata. *Nature*, **445**, 501–505.

Uchida, N., **Lee, J.S.**, **Horst, R.J.**, **Lai, H.-H.**, **Kajita, R.**, **Kakimoto, T.** *et al.* (2012) Regulation of inflorescence architecture by intertissue layer ligand-receptor communication between endodermis and phloem. *Proceedings of the National Academy of Sciences of the United States of America*, **109**, 6337–6342.

Uchida, N., **Shimada, M.** & **Tasaka, M.** (2013) ERECTA-family receptor kinases regulate stem cell homeostasis via buffering its cytokinin responsiveness in the shoot apical meristem. *Plant & Cell Physiology*, **54**, 343–351.

Van Zanten, M., **Basten Snoek, L.**, **Van Eck-Stouten, E.**, **Proveniers, M.C.G.**, **Torii, K.U.**, **Voesenek, L.A.C.J.** *et al.* (2010) Ethylene-induced hyponastic growth in *Arabidopsis thaliana* is controlled by ERECTA. *The Plant Journal*, **61**, 83–95.

Willige, B.C., **Ghosh, S.**, **Nill, C.**, **Zourelidou, M.**, **Dohmann, E.M.N.**, **Maier, A.** *et al.* (2007) The DELLA domain of GA INSENSITIVE mediates the interaction with the GA INSENSITIVE DWARF1A gibberellin receptor of Arabidopsis. *Plant Cell*, **19**, 1209–1220.

Wojtyla, Ł., **Rucińska-Sobkowiak, R.**, **Kubala, S.** & **Garnczarska, M.** (2013) Lupine embryo axes under salinity stress. I. Ultrastructural response. *Acta Physiologiae Plantarum*, **35**, 2219–2228.

Zentella, R., **Zhang, Z.-L.**, **Park, M.**, **Thomas, S.G.**, **Endo, A.**, **Murase, K.** *et al.* (2007) Global analysis of della direct targets in early gibberellin signaling in Arabidopsis. *Plant Cell*, **19**, 3037–3057.

Zhang, D., **Jing, Y.**, **Jiang, Z.** & **Lin, R.** (2014) The chromatin-remodeling factor PICKLE integrates Brassinosteroid and gibberellin signaling during Skotomorphogenic growth in Arabidopsis. *Plant Cell*, **26**, 2472–2485.

Zhang, L., **DeGennaro, D.**, **Lin, G.**, **Chai, J.** & **Shpak, E.D.** (2021) ERECTA family signaling constrains CLAVATA3 and WUSCHEL to the center of the shoot apical meristem. *Development*, **148**, dev189753.